

Inhibited carrier transfer in ensembles of isolated quantum dots

C. Lobo

Department of Electronic Materials Engineering, Research School of Physical Sciences and Engineering, Australian National University, Canberra ACT 0200, Australia

R. Leon

Jet Propulsion Laboratory, California Institute of Technology, Pasadena, California 91109

S. Marcinkevičius

Department of Physics-Optics, Royal Institute of Technology, S-100 44 Stockholm, Sweden

W. Yang and P. C. Sercel

Department of Physics and Materials Science Institute, University of Oregon, Eugene, Oregon

X. Z. Liao, J. Zou, and D. J. H. Cockayne

Australian Key Centre for Microscopy and Microanalysis, Electron Microscopy Unit, University of Sydney, Sydney NSW 2006, Australia

(Received 7 June 1999; revised manuscript received 16 August 1999)

We report significant differences in the temperature-dependent and time-resolved photoluminescence (PL) from low and high surface density $\text{In}_x\text{Ga}_{1-x}\text{As}/\text{GaAs}$ quantum dots (QD's). QD's in high densities are found to exhibit an Arrhenius dependence of the PL intensity, while low-density (isolated) QD's display more complex temperature-dependent behavior. The PL temperature dependence of high density QD samples is attributed to carrier thermal emission and recapture into neighboring QD's. Conversely, in low density QD samples, thermal transfer of carriers between neighboring QD's plays no significant role in the PL temperature dependence. The efficiency of carrier transfer into isolated dots is found to be limited by the rate of carrier transport in the $\text{In}_x\text{Ga}_{1-x}\text{As}$ wetting layer. These interpretations are consistent with time-resolved PL measurements of carrier transfer times in low and high density QD's. [S0163-1829(99)04748-7]

I. INTRODUCTION

Time-resolved and temperature-dependent photoluminescence (PL) measurements of quantum dot (QD) ensembles have helped to clarify the processes of energy relaxation and energy transfer in multiple and coupled quantum dot systems.¹⁻⁵ However, the influence of dot size and density on the luminescence energies and linewidths from QD ensembles is still not well understood, and the mechanisms involved in carrier relaxation and PL quenching seem strongly dependent on the material system, excitation conditions, and method of QD formation (self-assembled or strain-induced). It has recently been reported that the PL emission energies, inhomogeneous linewidths, intersublevel energies, and excited state relaxation times of ensembles of $\text{In}_x\text{Ga}_{1-x}\text{As}/\text{GaAs}$ QD's are strongly influenced by the QD density.⁶ Here we have investigated the luminescence emission from low density and high density $\text{In}_x\text{Ga}_{1-x}\text{As}/\text{GaAs}$ QD's by temperature-dependent and time-resolved PL. We find that the temperature dependence of the PL emission is determined primarily by the efficiency of carrier thermal transfer into the QD's. We also report differences in the degree of linewidth broadening of the PL emission from these low and high density QD's as a function of temperature. These differences result from the reduced influence of thermally activated carrier transfer and strain interaction as the average dot separation increases.

II. EXPERIMENTAL METHODS

QD structures of nominal composition $\text{In}_{0.6}\text{Ga}_{0.4}\text{As}$ were grown on slightly misoriented, semi-insulating $\text{GaAs}(100)$ substrates by metal organic chemical vapor deposition in a horizontal reactor cell operating at 76 Torr. The structures were grown under identical conditions, except for the AsH_3 partial pressure, which was varied in order to obtain widely differing densities of similar-sized $\text{In}_x\text{Ga}_{1-x}\text{As}$ islands.⁷ QD samples used for photoluminescence measurements were capped with 100 nm GaAs . Full details of the growth conditions are given in Ref. 7.

Average dot sizes in the capped samples used for PL measurements were determined by plan-view transmission electron microscopy (TEM) using a Phillips EM430 operating at 300 keV. Island concentrations were determined both by TEM of capped samples and by atomic force microscopy (AFM) of uncapped QD samples grown under identical conditions to the capped samples used for PL. Temperature dependent PL measurements were undertaken with above-band-gap excitation using a Ti:sapphire laser emitting at 804 nm pumped by an argon ion laser ($\lambda = 488$ nm), or directly using an argon ion laser. The signal was dispersed by a 0.25 m single grating monochromator and collected using a liquid- N_2 -cooled germanium detector. QD samples were mounted with indium to prevent sample heating. The average excitation power was 1 W/cm^2 .

Carrier transfer times into the QD's were measured by

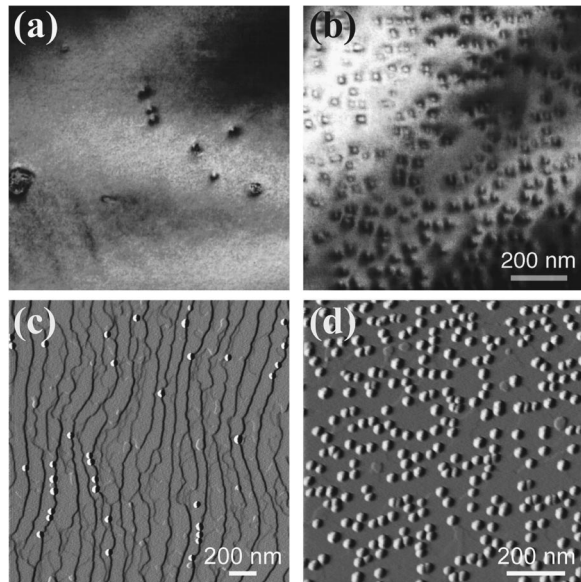


FIG. 1. Plan-view TEM images of capped samples used for PL measurements, and AFM images of uncapped samples grown under identical conditions. (a) Plan-view TEM image of isolated QD's with density $3.5 \times 10^8 \text{ cm}^{-2}$ (sample A). (b) Plan-view TEM image of interacting QD's with density $2.5 \times 10^{10} \text{ cm}^{-2}$. The scale applies to both TEM images. (c) $2 \times 2 \mu\text{m}^2$ AFM deflection image of isolated QD's with density $7 \times 10^8 \text{ cm}^{-2}$ (sample B). (d) $1 \times 1 \mu\text{m}^2$ AFM deflection image of interacting QD sample shown in (b). The average size of QD's in all three capped samples is $(25 \pm 5) \text{ nm}$.

time-resolved photoluminescence in the temperature range 80–300 K. A self-mode-locking Ti:sapphire laser (80 fs, 95 MHz, 800 nm) was used for excitation, and an upconversion technique with a temporal resolution of 150 fs used for signal detection. Excitation powers varied in the range 0.01 to 10 mW. The average excitation intensity for the temperature-dependent measurements was 10 W/cm^{-2} , which corresponds to approximately 2×10^{11} electron-hole pairs per square centimeter when spot size and reflections are taken into account.

III. TEMPERATURE-DEPENDENT PHOTOLUMINESCENCE

Figure 1 shows plan-view TEM and AFM images of representative high and low density QD samples. The low-density QD samples A and B [shown in Figs. 1(a) and 1(c), respectively] have nominal miscut angles of 0.25° and 0.75° off the (100) plane. These samples have dot densities of approximately $3.5 \times 10^8 \text{ cm}^{-2}$ and $7 \times 10^8 \text{ cm}^{-2}$. Average (edge to edge) QD separations are 280 nm in sample A and 190 nm in sample B. The high density QD sample shown in Fig. 1(b) and 1(d) is nominally on axis $[(100) \pm 0.05^\circ]$ and has an average dot density of $2.5 \times 10^{10} \text{ cm}^{-2}$ and an average QD separation of 10 nm. The average diameter of dots in all three capped samples is $(25 \pm 5) \text{ nm}$.

Low-temperature PL spectra from high and low density QD's are displayed in Fig. 2. Emission from the ground state and two excited states is observed from the low-density sample even under conditions of low excitation. This may be due to hindered intersublevel relaxation.^{8–10} In contrast, the high density QD's show only ground state emission under

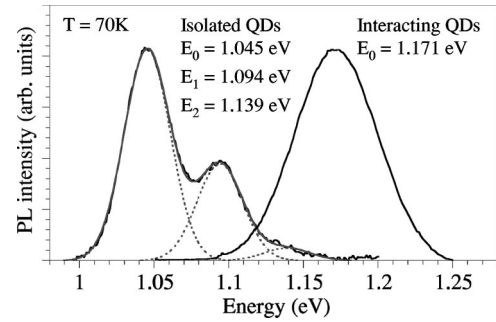


FIG. 2. Low-temperature (70 K) PL spectra of isolated and interacting QD's. The spectrum from the isolated QD's (sample A) is modeled as the sum of Gaussians with peak energies $E_0 = 1.045 \text{ eV}$, $E_1 = 1.094 \text{ eV}$, $E_2 = 1.139 \text{ eV}$, and $\Gamma = 21.8 \text{ meV}$.

continuous-wave (CW) excitation. The line shape of the PL emission from high-density QD's is unchanged with increasing excitation power.⁶ The high-density dots also exhibit a blueshift of the PL emission energy and a broadening of the ground-state inhomogeneous linewidth with respect to the low-density QD's at the same low temperature. These differences have been ascribed to progressive strain deformation of the QD confining potentials, which effectively result in shallower confinement as the dot density increases.⁶ The increased degree of strain interaction between neighboring high-density QD's, together with the randomness of these interactions, account for the observed differences in the CW PL. From here on these low- and high-density QD's will therefore be referred to as “isolated” and “interacting,” respectively.

A. Interacting QD's

The normalized PL intensity from interacting QD's is plotted as a function of temperature in Fig. 3. These QD's

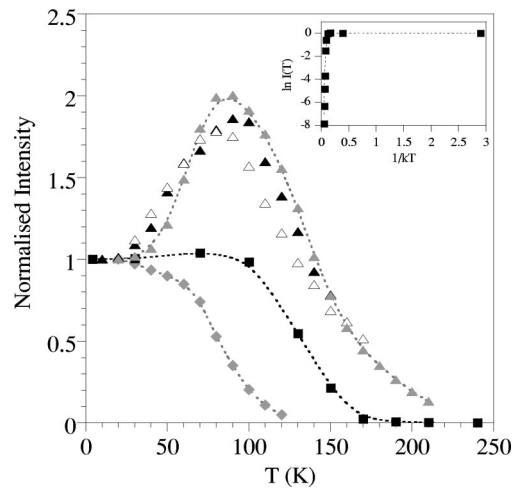


FIG. 3. Normalized integrated PL intensity as a function of temperature for several interacting and isolated QD samples. Isolated QD samples A and B are represented by filled gray and black triangles, respectively; PL data from a third sample is plotted with unfilled triangles. The integrated intensity from the $\text{In}_x\text{Ga}_{1-x}\text{As}$ WL in sample A is plotted with gray diamonds. PL data from the interacting QD's is plotted with black squares. The inset is an Arrhenius fit to the PL intensity from the interacting QD's as a function of temperature.

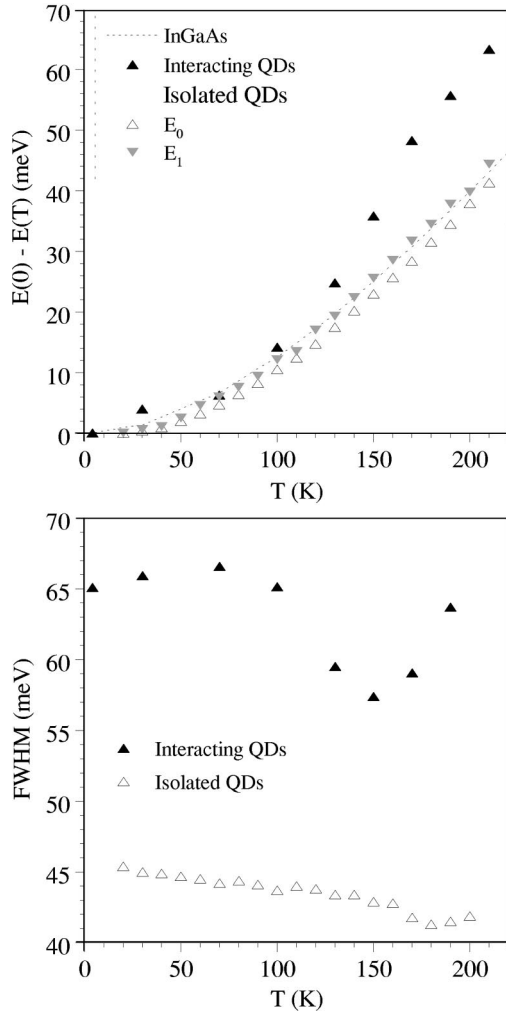


FIG. 4. (a) Redshift of the PL peak energy as a function of temperature for the interacting and isolated (sample A) QD's plotted with that of the $\text{In}_x\text{Ga}_{1-x}\text{As}$ free exciton emission. (b) Inhomogeneous linewidth broadening (FWHM) as a function of temperature for interacting and isolated (sample A) QD's.

exhibit the Arrhenius behavior typically observed for quantum wells^{11,12} (see inset, Fig. 3). The activation energy E_A extracted from these Arrhenius plots approximates the energy difference between the QD emission and that of the wetting layer (WL) or barrier. Emission from the WL in interacting QD samples is absent except at very low temperatures (< 20 K) or under high-excitation densities. Reported observations of a large increase in QD luminescence when the excitation energy exceeds the WL emission energy,¹³ and of an increase in the WL/QD intensity ratio with excitation power¹⁰ indicate that carriers are generated in the WL (and GaAs barrier) and subsequently transferred to the QD's. Hence, the lack of WL emission in CW PL indicates rapid carrier transfer from the WL to the high-density QD's.

The temperature dependencies of the PL redshift and inhomogeneously broadened linewidth (full width at half maximum, FWHM) of the QD emission are plotted in Fig. 4. The QD PL redshift is significantly greater than that of the $\text{In}_x\text{Ga}_{1-x}\text{As}$ free exciton emission¹⁴ at temperatures above 100 K. The FWHM of the QD PL emission first decreases and then increases over an 8 meV range with increasing temperature. Similar dependencies of the energy shift and

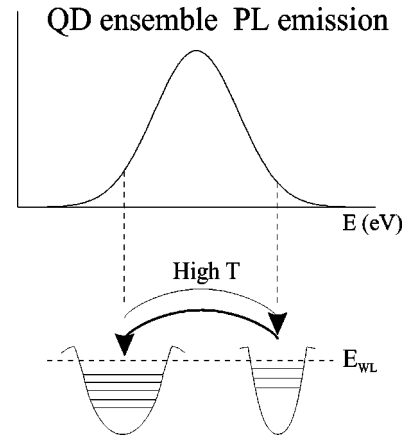


FIG. 5. Schematic of thermally activated carrier transfer between neighboring quantum dots in high-density QD structures.

FWHM of the QD PL peak on temperature have been reported previously¹⁵⁻¹⁷ and attributed to the effects of thermal activation transfer and tunneling transfer between neighboring QD's (see Fig. 5). At low temperatures, there is no significant thermal emission of carriers out of the QDs. Hence, the PL redshift of the QD peak is equivalent to that of the $\text{In}_x\text{Ga}_{1-x}\text{As}$ band gap and the FWHM remains constant. Above ≈ 100 K, carrier thermal emission out of the smaller QD's in the ensemble and recapture by neighboring QD's with deeper confining potentials becomes significant. This behavior explains the simultaneous redshifting and narrowing of the PL peak. At higher temperatures (above ≈ 150 K) the FWHM increases and the rate of redshift decreases as thermal emission of carriers out of the larger QD's (and recapture by all dots) in the ensemble becomes significant. Filling of the excited states of the larger dots in the ensemble may also contribute to the broadening of the FWHM observed at high temperature. Tunneling of carriers between neighboring QD's may play a role, although this process is independent of temperature and would lead to a reduction of the FWHM across the whole temperature range. Attempts to model the observed behavior by accounting only for carrier thermal transfer between neighboring QD's have been only partially successful.^{15,16} In particular the FWHM at high T is often greater than that at low T , an observation that cannot be explained by a simple thermionic emission model. A successful model may require inclusion of the effects of excited state filling and varying strain interactions between neighboring QD's.

B. Isolated QD's

PL emission from the ground and excited states of the isolated QD's can be modeled by Gaussians with a constant inhomogeneous broadening factor ($\Gamma = 1/2\text{FWHM}$) and level spacings of 45–50 meV.¹⁰ The integrated PL intensity, energy shift, and FWHM extracted from these fits to the PL spectra are plotted as a function of temperature in Figs. 3 and 4. The integrated intensity of the luminescence emission from the ground and excited states increases from 20–90 K, and subsequently decreases up to 210 K (see Fig. 3). The total PL intensity at 90 K is approximately twice the low-temperature value. At low temperature, the wetting layer emission is more intense than the QD emission. The inte-

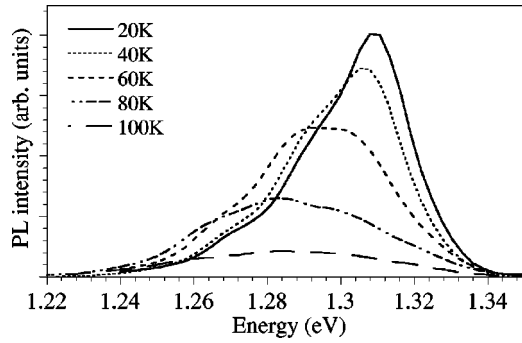


FIG. 6. Luminescence emission from the wetting layer in isolated QD sample A at several temperatures.

grated intensity of the WL emission as a function of temperature is also plotted in Fig. 3. This plot shows that the wetting layer emission obeys the Arrhenius dependence observed for quantum wells.^{11,12}

Wetting layer emission spectra obtained at a number of temperatures are shown in Fig. 6. The line shape of the broad WL emission changes with increasing temperature. The intensity of the low-energy tail increases relative to the high-energy tail, indicating the existence of potential fluctuations in the WL. Such fluctuations may be caused by indium segregation and enrichment in the quantum dots,¹⁸ which would produce gallium-rich regions in the WL. Variations in strain induced by the QD's would also produce regions of lateral confinement in the WL.¹⁰ The observed change in the line shape of the WL emission with increasing temperature indicates that some carriers thermally emitted from regions of the WL with shallow confining potentials are retrapped and recombine in regions of deeper confinement. This behavior is analogous to retrapping of carriers thermally emitted from shallow wells by adjacent deeper wells in multiple quantum well samples.¹⁹

It has been established that carrier transfer to these $\text{In}_x\text{Ga}_{1-x}\text{As}/\text{GaAs}$ quantum dots occurs via the WL.^{10,13} The WL behaves as a reservoir of carriers, available to the QD's provided the two-dimensional (2D) diffusion length in the WL is long enough for capture into the QD's to occur prior to recombination in the WL. In high-density QD's, the absence of a WL emission in CW PL indicates that the average dot-dot separation is shorter than the carrier diffusion length in the WL.¹⁰ The carrier mobility in the WL would be expected to play a greater role in the rate of carrier transfer to the QD's as the average dot-dot separation increases.

We attribute the increase in PL intensity from isolated QD's (Fig. 3) to carrier transfer mechanisms in the WL. At elevated temperatures, carriers trapped at potential fluctuations in the WL may acquire sufficient thermal energy to overcome these barriers. Such an increase in carrier thermal transfer within the WL would result in an increased rate of carrier capture by the QD's and produce the observed increase in QD PL intensity. The rate of carrier transfer to the QD's is also limited by the rate of lateral transport in the $\text{In}_x\text{Ga}_{1-x}\text{As}$ WL, which for photoexcited carriers is governed by hole diffusion. Hole mobility in $\text{In}_x\text{Ga}_{1-x}\text{As}$ increases with temperature up to ≈ 100 K.²⁰ This increase in hole mobility may increase the rate of carrier capture into the QD's and therefore contribute to the observed increase in QD PL intensity. At temperatures greater than 100 K, ther-

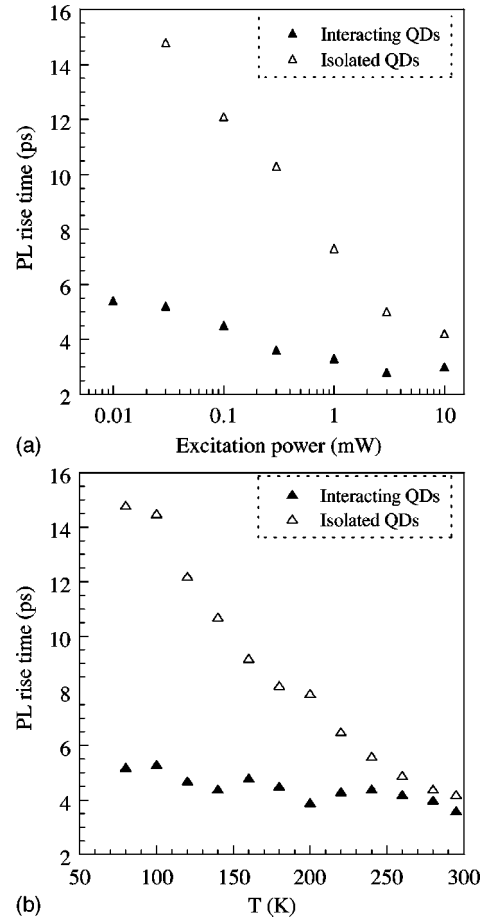


FIG. 7. PL rise times as a function of (a) excitation power and (b) temperature for interacting and isolated (sample B) QD's.

mal emission of carriers from the QD's becomes dominant. The QD PL intensity therefore follows an approximately exponential decrease up to room temperature.

The PL redshift of the emission from the ground state and first excited state of the isolated QD's is plotted as a function of temperature in Fig. 4. The redshift of both emissions follows that of the $\text{In}_x\text{Ga}_{1-x}\text{As}$ free exciton emission with increasing temperature. The inhomogeneously broadened linewidth of the isolated QD's shows an approximately linear decrease from 45 to 41 meV over the temperature range 10–210 K. We attribute these behaviors to thermal emission of carriers from the smaller QD's in the ensemble without subsequent recapture by larger QD's. Thus carrier transfer between neighboring QD's has no significant effect on the PL temperature dependence.

IV. TIME-RESOLVED PHOTOLUMINESCENCE

Carrier transfer in isolated and interacting quantum dot samples was also investigated by time-resolved photoluminescence. The rise times of the luminescence emission from the isolated and interacting QD's have been studied as a function of excitation intensity and temperature (see Fig. 7). These rise times were measured at the ground state PL peak energies, and account for carrier transport, capture and relaxation in the QD's. Fast carrier transfer into the interacting QD's is confirmed by the short PL rise times shown in Fig. 7. The rise times for interacting QD's show a slight decrease

with increasing excitation power and display no significant dependence on temperature. The magnitudes and behavior of the PL rise times for interacting QD's are very similar to those observed for quantum wells of similar composition.²¹

For the isolated QD's, the PL rise times decrease from 15 to 5 ps with increasing excitation power from 0.01 to 10 mW, and increasing temperature from 80 to 300 K. The excitation power dependence may be explained by a reduced importance of diffusion limited transport at high carrier densities. As the excitation power increases, a greater number of carriers are generated in the vicinity of the isolated QD's. Hence, the PL rise time of the isolated QD's approaches that of the interacting QD's at very high-excitation densities. Potential barriers around the isolated QD's induced by band bending²² would also be reduced at high-carrier densities due to screening of the internal electric field.²³ The decrease of the PL rise time with temperature is consistent with an increased rate of carrier transfer due to carriers having greater thermal energy to overcome these potential barriers around the QD's or in the WL.

The temperature and excitation power dependence of the rise times of the PL emission from isolated QD's confirm the interpretation of the PL temperature dependence in terms of carrier transfer mechanisms in the WL. Further studies will be undertaken on InAs QD's, in which the effects of indium segregation and enrichment in the QD's and associated com-

positional fluctuations in the WL would be minimized.²⁴ Differences in the PL temperature dependence of In_xGa_{1-x}As/GaAs and InAs/GaAs QD's may clarify the effects of temperature-dependent hole mobility and potential fluctuations in the WL on carrier transfer to isolated quantum dots.

V. CONCLUSION

In conclusion, we have conducted a study of the temperature-dependent and time-resolved PL from interacting and isolated In_xGa_{1-x}As quantum dots. We find that for high-density QD samples, the temperature dependence of the PL emission is determined by carrier thermal emission and recapture into neighboring QD's. In low-density QD's the efficiency of carrier transfer into the dots is limited by the rate of carrier transport in the In_xGa_{1-x}As wetting layer. Thermal transfer of carriers between neighboring QD's plays no significant role in the PL temperature dependence.

ACKNOWLEDGMENTS

C.L. thanks C. Jagadish for helpful discussions. Part of this work was sponsored by the Australian Research Council and by the Jet Propulsion Laboratory, under a contract with the National Aeronautics and Space Administration.

-
- ¹G. Wang, S. Fafard, D. Leonard, J. E. Bowers, J. L. Merz, and P. M. Petroff, *Appl. Phys. Lett.* **64**, 2815 (1994).
- ²S. Raymond, S. Fafard, P. J. Poole, A. Wojs, P. Hawrylak, S. Charbonneau, D. Leonard, R. Leon, P. M. Petroff, and J. L. Merz, *Phys. Rev. B* **54**, 11 548 (1996).
- ³W. Yang, R. Lowe-Webb, H. Lee, and P. C. Sercel, *Phys. Rev. B* **56**, 13 314 (1997).
- ⁴M. Braskén, M. Lindberg, M. Sopanen, H. Lipsanen, and J. Tulkki, *Phys. Rev. B* **58**, R15 993 (1998).
- ⁵Y. Zhang, M. D. Sturge, K. Kash, B. P. van der Gaag, A. S. Gozdz, L. T. Florez, and J. P. Harbison, *Superlattices Microstruct.* **17**, 201 (1995); *Phys. Rev. B* **51**, 13 303 (1995).
- ⁶R. Leon, S. Marcinkevičius, X. Z. Liao, J. Zou, D. J. H. Cockayne, and S. Fafard, *Phys. Rev. B* **60**, R8517 (1999).
- ⁷R. Leon, C. Lobo, J. Zou, T. Romeo, and D. J. H. Cockayne, *Phys. Rev. Lett.* **81**, 2486 (1998).
- ⁸H. Benisty, C. M. Sotomayor-Torrès, and C. Weisbuch, *Phys. Rev. B* **44**, 10 945 (1991).
- ⁹U. Bockelmann, *Phys. Rev. B* **48**, 17 637 (1993).
- ¹⁰R. Leon, S. Fafard, P. G. Piva, S. Ruvimov, and Z. Liliental-Weber, *Phys. Rev. B* **58**, R4262 (1998).
- ¹¹J. D. Lambkin, D. J. Dunstan, K. P. Homewood, L. K. Howard, and M. T. Emeny, *Appl. Phys. Lett.* **57**, 1986 (1990).
- ¹²G. Bacher, H. Schweizer, J. Kovac, A. Forchel, H. Nickel, W. Schlapp, and R. Lösch, *Phys. Rev. B* **43**, R9312 (1991).
- ¹³S. Fafard, D. Leonard, J. L. Merz, and P. M. Petroff, *Appl. Phys. Lett.* **65**, 1388 (1994).
- ¹⁴S. Paul, J. B. Roy, and P. K. Basu, *J. Appl. Phys.* **69**, 827 (1991).
- ¹⁵S. Fafard, S. Raymond, G. Wang, R. Leon, D. Leonard, S. Charbonneau, J. L. Merz, P. M. Petroff, and J. E. Bowers, *Surf. Sci.* **362**, 778 (1996).
- ¹⁶Z. Y. Xu, Z. D. Lu, Z. L. Yuan, X. P. Yang, B. Z. Zheng, J. Z. Xu, W. K. Ge, Y. Wang, J. Wang, and L. L. Chang, *Superlattices Microstruct.* **23**, 381 (1998).
- ¹⁷A. Patané, M. Grassi Alessi, F. Intonti, A. Polimeni, M. Capizzi, F. Martelli, M. Geddo, A. Bosacchi, and S. Franchi, *Phys. Status Solidi A* **164**, 493 (1997).
- ¹⁸X. Z. Liao, J. Zou, D. J. H. Cockayne, R. Leon, and C. Lobo, *Phys. Rev. Lett.* **82**, 5148 (1999).
- ¹⁹M. Vening, D. J. Dunstan, and K. P. Homewood, *Phys. Rev. B* **48**, 2412 (1993).
- ²⁰The hole mobility in In_xGa_{1-x}As peaks between 70 and 100 K, depending on the relative contributions of ionized impurity scattering, polar optical phonon scattering, acoustic phonon scattering, and alloy scattering [see S. Adachi, *Physical Properties of III-V Semiconductor Compounds* (Wiley, New York, 1992)].
- ²¹S. Marcinkevičius and R. Leon, *Phys. Rev. B* **59**, 4630 (1999).
- ²²B. K. Ridley, *Phys. Rev. B* **50**, 1717 (1994).
- ²³G. C. Crow and R. A. Abram, *Semicond. Sci. Technol.* **14**, 1 (1999).
- ²⁴J. Tersoff, *Phys. Rev. Lett.* **81**, 3183 (1998).